Supporting Information

Experimental details

The Ferrocene powder was vacuum-sealed in a Borosilicate glass ampule and then annealed in a furnace that was rapidly elevated to 550 – 750 °C. Self-organisation properties of ferrocene in the ampule were studied at various maximum temperatures (T_M °C) and densities of ferrocene precursor (ρ_0 mol m^{-3}). Within our target range of temperature and precursor density, ferrocene stays within a pressure range of 10 – 100 atoms, which is well below the saturation pressures extrapolated from the reference data (*1*), and therefore, the ideal gas law can be applied. In this case, the effective pressure $p = R(T_M + 273.15)\rho_0$ MPa, where $R = 8.314 \times 10^{-6}$ m^3 MPa K^{-1} mol^{-1} is the gas constant, effectively defines the pressure of ferrocene. The synthesis process includes a rapid increase of the furnace temperature up to T_M, kept for 0 – 1 h, followed by cooling down to room temperature. Holding time at T_M is found insignificant to the selection of emerging symmetry.

Scanning electron microscopy (SEM) images were obtained using a FEI Quanta 200F ESEM. Transmission electron microscopy (TEM) samples were prepared using a FEI Nova Nanolab 600 Dual Beam Microscope that combines a high-resolution field emission SEM with a focused ion beam (FIB) for etching and deposition. The micro-cones are first covered in the FIB with $\sim$1 μm of tungsten deposit and are ion milled at 500 pA for the initial thinning and then thinned further and finally polished at 30 pA. A Hitachi HD-2300A Scanning Transmission Electron Microscope (Schottky Field emitter, 200 keV) was used for bright-field and Z-contrast (probe diameter $\sim$3Å) and nano-diffraction (probe diameter $\sim$1 nm). A Phillips CM200ST Transmission Electron Microscope (LaB6 emitter, 200 keV) fitted with a Gatan Imaging Filter (GIF2001) was used for Energy-Filtered TEM images.

Measurement details

In Figure S2(a), we show how the length, diameter and angle of the samples is calculated for a specific sample.

The length of L of the samples is calculated by adding the lengths of all the line segments that closely follow the middle of the sample, as shown in Figure S2(a) and (b). The diameter D is the diameter of the core. There is a linear relationship between the length and diameter of the core, as shown in Figure 3 of the main paper of $L \approx 4.3D$.

The linear relationship between L and D means that a cone angle can be defined, as shown in Figure S2(a). The cone angle is found by fitting two straight lines to the cone profile. The cone angle is the angle between these two lines and can be found from the gradients of the two lines. The mean cone angle was found to be 0.18 ± 0.09 radians.

Symmetry breaking on the surface of a sphere

Symmetry breaking theory allows one to predict the symmetry of new states or structures near onset due solely to the geometry of the problem. Such is the strength of geometry on a problem that it has led many mathematicians to provide a general theory for symmetry breaking for different geometries (*2, 3*). The subject has always been led by physical examples of symmetry breaking starting with the pioneering work of Alan Turing in 1952 on morphogenesis of an embryo cell into a ball of cells (*4*) to across the physical (*5, 6*) and life sciences (*7, 8*). Crucially, the mathematics tells us that the geometry of a particular problem determines the symmetry and from the symmetry alone much can then be deduced on what patterns can exist and what transitions between different patterns are the most likely to occur. The precise physics or chemistry then determines quantitative details such as when particular transitions actually occur.

In our experiment, we suppose that iron and carbon start to aggregate to form a uniform spherical iron-rich core. As the core grows, more iron and carbon accumulate flowing round and through the core. In this initial phase, the carbon is uniformly distributed over the surface and the core has spherical symmetry. Once the core reaches a critical state, there is a spontaneous symmetry breaking bifurcation to a state which no longer has a uniform distribution of carbon on the surface. It is this non-uniform distribution of carbon that then results in the growing arms.

Understanding the flow of carbon atoms over/through a small spherical iron-rich core in our experiment, has mathematical analogies with continental drift via convection of magma near the surface (*9*) and tumour growth where a ball of cells goes from being spherical to non-spherical (*10, 11*). In all cases, the initial starting point is a small sphere (the uniform state) which has $O(3)$ symmetry. When this uniform state undergoes spontaneous symmetry breaking then the mathematics says that a new, small amplitude, solutions emerge from the uniform state that maybe described by the spherical equivalent of a Fourier series of a physical scalar quantity (for example density of carbon)

$$u = \sum_{m=-l}^{l} z_m(t) Y_l^m(\theta, \phi),$$

where z_0 is real, z_m is complex for $m \neq 0$ and Y_l^m are spherical harmonics. Since u is a real quantity, $z_{-m} = (-1)^m z_m^*$. The particular value of l depends on the physics of the problem: l is roughly proportional to the size of the sphere compared with the wavelength of the instability, so for example, for convection on a spherical shell, the 'thicker' the convecting layer as compared to the radius of the sphere, the lower the value of l. Initially, all states are unstable, however, for a given l it is possible to determine the least unstable state to emerge and it this state that is the most likely state to be seen experimentally (*12, 13*).

In our experiment, the radius of the spiral tips suggests that the transition from uniform/non-uniform growth occurs when the core is very small and carbon flows through the bulk. In turn, this suggests that l will be small. For $l = 2$ the expected state is an axisymmetric state, as shown in Figure 1 of the letter. This axisymmetric state would result in the formation of two arms.

After this initial onset of the axisymmetric state, we expect further symmetry breaking leading to the non-symmetric growth patterns shown in Figure 2 of the letter.

Modelling carbon cones and spirals

Once the axisymmetric state is created via symmetry breaking, two symmetric arms emerge from a growing core. To gain further insight into this process we model the arms using the geometry of the growth and conservation of mass.

Our modelling of the formation of the arms provides the basis for further work in modelling carbon growth from a catalyst or substrate. The high accuracy of the predictions from our model without requiring parameter fitting, makes this modelling particularly appealing.

The Ferrocene compound $Fe(C_5H_5)_2$ is heated up in a furnace to approximately 600°C where it dissociates to form a cementite (Fe_3C) core and polycrystalline graphite arms. We then suppose that the number of cementite molecules in the core at anytime is $N_C(t)$ and the cementite molecules accumulate at a constant rate k_C, so

$$\frac{dN_C}{dt} = k_C.$$

Similarly, we suppose that the number of graphite atoms in the arms at anytime is $N_A(t)$ and that the graphite accumulates at a constant rate k_A, then

$$\frac{dN_A}{dt} = k_A.$$

We now calculate how the radius of the core grows as a function of time. Since each cementite molecule causes a change in volume v_C, then the rate of change of volume of the core is given by

$$\frac{dV_C}{dt} = v_C \frac{dN_C}{dt} = v_C k_C.$$

Since the core is approximately spherical, $V_C(t) = 4\pi R(t)^3/3$ we get

$$\frac{dV_C}{dt} = 4\pi R^2 \frac{dR}{dt} = v_C k_C. \tag{1}$$

We note that the core appears to be more ellipsoidal but we would still expect the volume to be proportional to R^3 (but with a different proportionality constant). We solve (1) with the initial condition $R(0) = 0$ at time zero, to get

$$R = \left(\frac{3 v_C k_C}{4\pi} t \right)^{\frac{1}{3}}. \tag{2}$$

We now use this equation for the radius to describe the growth of the arms. Each graphite atom induces a change in the volume v_A and so we can calculate the rate of change of volume of a single arm as

$$\frac{dV_A}{dt} = \frac{1}{2} v_A \frac{dN_A}{dt} = \frac{1}{2} v_A k_A,$$

where the factor of a half is due to half the the graphite going into one arm. An incremental change in the volume of an arm δV_A is related to changes in the radius and length of the arm,

$$\delta V_A \approx \pi R^2 \delta L_{th}.$$

Hence, we find

$$\frac{dV_A}{dt} = \pi R^2 \frac{dL_{th}}{dt} = \frac{1}{2} v_A k_A \qquad \Rightarrow \frac{dL_{th}}{dt} = \frac{v_A k_A}{2\pi R^2}.$$

Using equation (2), we can solve the differential equation for L_{th} with $L_{th}(0) = 0$ at time zero to find

$$L_{th} = \left(\frac{6}{\pi}\right)^{\frac{1}{3}} \cdot \frac{v_A k_A}{(v_C k_C)^{\frac{2}{3}}} t^{\frac{1}{3}} \tag{3}$$

Dividing equation (3) by the equation for the radius (2), yields the relation

$$L_{th} = 2 \frac{v_A}{v_C} \frac{k_A}{k_C} R.$$

Note that this indicates that the arms will have a conical shape with a cone angle given by

$$\theta = 2\arctan\left(\frac{1}{2} \frac{v_C}{v_A} \frac{k_C}{k_A}\right).$$

From the TEM scans, we know the arms are almost pure graphite while the core is made up of cementite. This gives us a ratio of 1:29 molecules in the core to arms, i.e., $k_C/k_A = 1/29$. From crystallographic data (Unit cell $Fe_{12}C_4$, volume 151.73Å^3 (*14*)) the molar volume of Fe_3C is v_C=22.83cm^3/mol while for polycrystalline graphite the molar volume is v_A=5.29cm^3/mol.

Equations (2) and (3) are used together with an equation for the spiralling, to create the sketch of the micro-spirals in Figure 3 of the letter.

References and Notes

1. M. J. S. Monte, L. M. N. B. F. Santos, M. Fulem, J. M. S. Fonseca, C. A. D. Sousa, *J. Chem. Eng. Data* **51**, 757 (2006).

2. M. Golubitsky, D. G. Schaeffer, *Singularities and groups in bifurcation theory. Vol. I*, vol. 51 of *Applied Mathematical Sciences* (Springer-Verlag, New York, 1985).

3. M. Golubitsky, I. Stewart, D. G. Schaeffer, *Singularities and groups in bifurcation theory. Vol. II*, vol. 69 of *Applied Mathematical Sciences* (Springer-Verlag, New York, 1988).

4. A. M. Turing, *Philos. Trans. R. Soc. Lond. Ser. B-Biol. Sci.* **237**, 37 (1952).

5. V. V. Belkov, *et al.*, *Nature* **397**, 398 (1999).

6. C. Harrison, *et al.*, *Science* **290**, 1558 (2000).

7. S. Basu, Y. Gerchman, C. H. Collins, F. H. Arnold, R. A. Wiess, *Nature* **434**, 1130 (2005).

8. K. Hirose, K. Shiro, M. Tanabe, H. Takeshima, M. Iino, *Science* **284**, 1527 (1999).

9. F. H. Busse, *Journal of Fluid Mechanics* **72**, 67 (1975).

10. H. Byrne, P. C. Matthews, *IMA J. Math. Appl. Med. Biol.* **19**, 1 (2002).

11. M. A. J. Chaplain, M. Ganesh, I. G. Graham, *J. Math. Biol.* **42**, 387 (2001).

12. P. C. Matthews, *Nonlinearity* **16**, 1449 (2003).

13. P. C. Matthews, *Phys. Rev. E* **67** (2003).

14. C. Jiang, S. G. Srinivasan, A. Caro, S. A. Maloy, *J. Appl. Phys.* **103**, 043502 (2008).

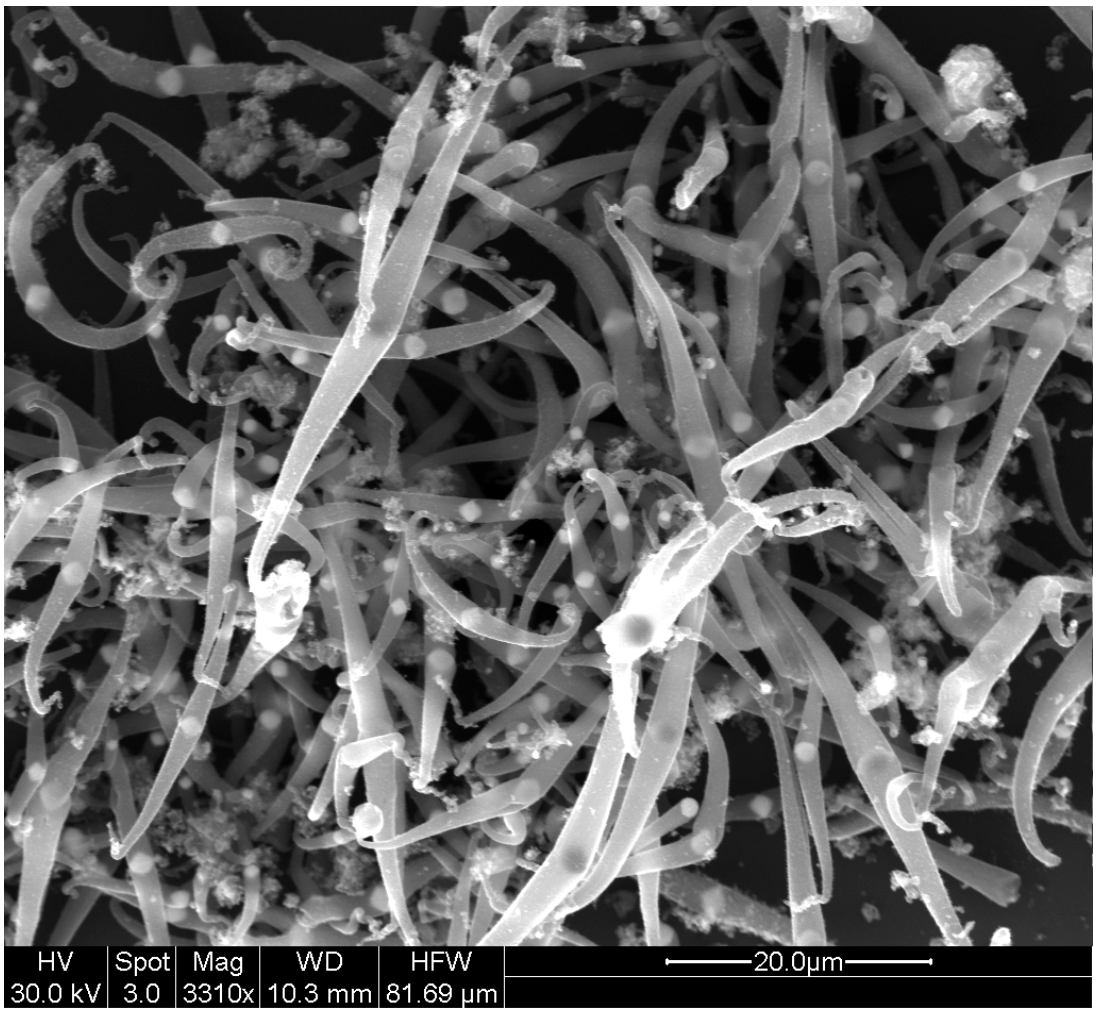

Figure S1: **Large-scale scanning electron micrograph, showing the micro-cones produced in high yield at 6.1 MPa.**

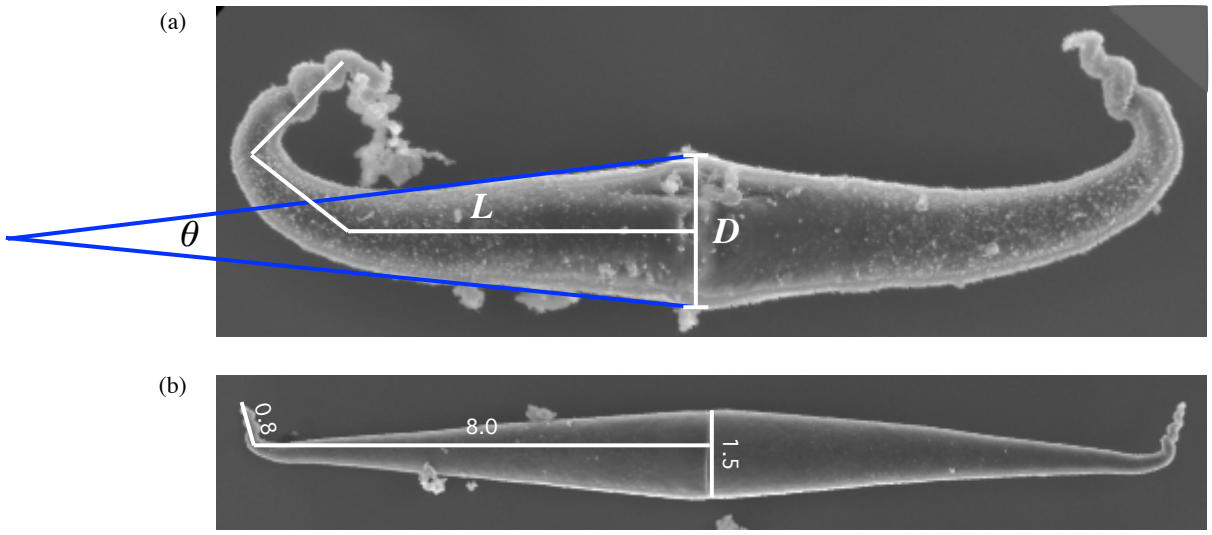

Figure S2: **(a) The measurement of the length, diameter and angle for a single microstructure. For this sample it is found that $L \approx 3.9D$ with an angle of $\theta \approx 0.22$. We note that the true length of the sample is very close to that of the distance of the intersection point for the angle lines from the centre of the structure suggesting $L \approx 4.5D$. (b) a sample with relative lengths shown. For this sample $L \approx 6D$ which is close to the theoretical value of $L_{th} \approx 6.7D$.**